Modeling the Transfer of Drug Resistance in Solid Tumors

Matthew Becker · Doron Levy

Received: date / Accepted: date

Abstract ABC efflux transporters are a key factor leading to multidrug resistance in cancer. Overexpression of these transporters significantly decreases the efficacy of anti-cancer drugs. Along with selection and induction, drug resistance may be transferred between cells, which is the focus of this paper. Specifically, we consider the intercellular transfer of P-glycoprotein (P-gp), a well-known ABC transporter that was shown to confer resistance to many common chemotherapeutic drugs.

In a recent paper, Durán *et al.* studied the dynamics of mixed cultures of resistant and sensitive NCI-H460 (human non-small lung cancer) cell lines [9]. As expected, the experimental data showed a gradual increase in the percentage of resistance cells and a decrease in the percentage of sensitive cells. The experimental work was accompanied with a mathematical model that assumed P-gp transfer from resistant cells to sensitive cells, rendering them temporarily resistant. The mathematical model provided a reasonable fit to the experimental data.

In this paper we develop a new mathematical model for the transfer of drug resistance between cancer cells. Our model is based on incorporating a resistance phenotype into a model of cancer growth [14]. The resulting model for P-gp transfer, written as a system of integro-differential equations, follows the dynamics of proliferating, quiescent, and apoptotic cells, with a varying resistance phenotype. We show that this model provides a good match to the dynamics of the experimental data of [9]. The mathematical model further suggests that resistant cancer cells have a slower division rate than the sensitive cells.

Keywords P-glycoprotein · Multidrug Resistance · Integro-Differential Equations

M. Becker

Department of Mathematics, University of Maryland, College Park, Maryland, 20742, USA E-mail: mhbecker@math.umd.edu

D. Levy

Department of Mathematics and Center for Scientific Computation and Mathematical Modeling (CSCAMM), University of Maryland, College Park, Maryland, 20742, USA E-mail: dlevy@math.umd.edu

1 Introduction

Antineoplastic resistance is often the key impediment to effective cancer treatment. Though advances in early detection have increased survival rates across several cancer subtypes, resistance to chemotherapy is prevalent [1,12], and the majority of patients will relapse at a certain point following treatment. Therapeutic failure may be attributed to intrinsic tumor heterogeneity prior to therapy (e.g., spatial localization of cancer cells within a tumor, initial cellular genetic landscape, cell-cycle length variations, etc.) or induced tumor heterogeneity after initiation of therapy, such as altered molecular signaling, genetic modification, and microenvironmental alterations.

Development of resistance to one drug can also lead to resistance to other structurally and mechanistically unrelated drugs, a phenomenon referred to as multidrug resistance (MDR). MDR can be understood through different biological factors and is often identified with drug efflux [10]. There has been increasing evidence that drug cellular uptake is regulated by transport proteins expressed on the cellular membrane, which are responsible for drug transport across the plasma membrane and throughout the cell. One such example is the family of ABC (ATP Binding Cassette) transporters. ABC transporters can pump away chemotherapeutic agents, which allow certain cells to withstand the drugs' cytotoxic effect [13]. These non drug-specific transporters provide a mechanism for the cells to resist unrelated drugs, which then leads to a chemotherapy breakdown. While ABC transporters have important roles in the importation of nutrients and exportation of toxic molecules [8], their overexpression is a serious obstacle in anti-cancer therapies.

P-glycoprotein (P-gp), a product of the ABCB1 (*mdr1*) gene, is a well-known ABC transporter that correlates with MDR [19,25]. It has been shown to confer resistance to many common chemotherapeutic drugs [4,7,11,16]. In normal human tissues it is concentrated in cells in the liver, pancreas, kidney, colon, and jejunum [24]. The MDR1 gene encodes the transmembrane P-gp pump that cells use to excrete structurally and chemically diverse drugs [26]. A drug molecule is bound by the P-gp's cytoplasmic domain; the protein subsequently uses ATP hydrolysis and opens itself to the extracellular space and expels the drug molecule [26]. The overexpression of P-gp can lead to resistance of more than 100 times higher than normal cells [5].

Drug resistance is often a multifactorial, complex process that arises through a series of genetic and non-genetic changes across multiple cancers. Such changes can be the consequence of drug administration (therapy-dependent), or can be acquired independently of any drug (therapy-independent). The focus of this work is on drug resistance that may be transferred between cells, e.g., via cell-to-cell communication. Two studies in 2005 showed resistant populations can spread their resistance to sensitive cells [2,20]. More recently, intracellular membrane nanotubes were shown to carry P-gp between neighboring cells [22].

Mathematicians have previously studied MDR in correlation with tumor heterogeneity [15,18,17,21]. Jackson & Byrne used a PDEs model to describe the reduction of volume in vascularized tumors with discrete sensitive and resistant cells [15]. Lorz *et al.* [21] modeled resistance as a continuous variable and demonstrated that the presence of a cytotoxic agent leads to diminished heterogeneity and a population of overwhelmingly resistant cells. Lavi *et al.* extended the approach of Lorz to model

intratumoral heterogeneity [18]. For a review on mathematical models of MDR we refer to [17] and the references therein.

Relatively little attention has been given in the mathematical community to modeling the transfer of drug resistance between cells. Pasquier *et al.* [23] studied cell-to-cell transfers of P-gp in co-cultures combining a sensitive human breast cancer MCF-7 cell line, and a P-gp overexpressed variant, selected for its resistance towards doxorubicin. Pasquier *et al.* derived a Boltzmann type integro-partial differential equation structured by a continuum variable corresponding to P-gp activity. The model was used to quantify the transfer of P-gp activity and, in conjunction with the experimental data, to confirm the cell-to-cell transfer of functional P-gp.

A more recent work by Durán *et al.* [9], derived two models for P-gp transfer assuming P-gp expression has a discrete characteristic: P-gp in a cell is either overexpressed or not. These models are written as a coupled system of ordinary differential equations (ODEs) describing the behavior of sensitive cells (S), resistant cells (R), and temporarily resistant cells (S_R). Interaction between sensitive and resistant cells allows the resistant population to transfer P-gp to the sensitive cells, which become temporarily resistant. Since this is a phenotypic change, the progenies of these cells revert back to a sensitive state. The resistant cells are not affected by the interaction and exhibit logistic growth. The first model of [9] is given by

$$\frac{dS}{dt} = \frac{S}{\tau_s} \left(1 - \frac{R + S + S_R}{K} \right) - \frac{SR}{\tau_c} + \frac{S_R}{\tau_*},\tag{1a}$$

$$\frac{dR}{dt} = \frac{R}{\tau_r} \left(1 - \frac{R + S + S_R}{K} \right),\tag{1b}$$

$$\frac{dS_R}{dt} = \frac{S_R}{\tau_r} \left(1 - \frac{R + S + S_R}{K} \right) + \frac{SR}{\tau_c} - \frac{S_R}{\tau_*}. \tag{1c}$$

We note that this model, while separating sensitive, resistant, and temporary-resistant cells, does not explicitly assume any drug action.

A second model proposed in [9] extends (1) by assuming that P-gp is transfered through the shedding of microvessicles (MVs) by resistant cells. MVs are small particles that are released via plasma membrane blebbing. In addition to their role in mediating inflammation, coagulation, and vascular homeostasis, they are important mediators of MDR, as they facilitate cell-to-cell communication and can deliver proteins between cells [3]. The intake of MVs by sensitive cells may lead to temporary resistance. A system of ODEs that incorporates the role of MVs (*Q*) in mediating MDR is written in [9] as

$$\frac{dS}{dt} = \frac{S}{\tau_s} \left(1 - \frac{R + S + S_R}{K} \right) - \frac{QS}{\tau_{\eta}} + \frac{S_R}{\tau_*}, \tag{2a}$$

$$\frac{dR}{dt} = \frac{R}{\tau_r} \left(1 - \frac{R + S + S_R}{K} \right),\tag{2b}$$

$$\frac{dS_R}{dt} = \frac{S_R}{\tau_r} \left(1 - \frac{R + S + S_R}{K} \right) + \frac{QS}{\tau_\eta} - \frac{S_R}{\tau_*}, \tag{2c}$$

$$\frac{dQ}{dt} = \lambda_1 R - \lambda_2 S\left(\frac{Q}{Q_{th} + Q}\right). \tag{2d}$$

In addition to introducing the mathematical models, Durán *et al.* conducted experiments on mixed cultures of NCI-H460 cell line (human non-small cell lung carcinoma) cells and NCI-H460/R resistant cells that were selected from NCI-H460 cells after three months of doxorubicin selective pressure. Cultures of only sensitive, only resistant, and mixed cultures were seeded in ratios 1:1, 3:1, and 7:1 sensitive to resistant cells and their growth was followed over time. Flow cytometry was used to measure P-gp expression levels at time points 0, 24, 48, 72, and 96 hours, and P-gp transfer was analyzed every 24 hours. The experimental data was used to calibrate the parameters of the mathematical models.

In Fig. 1 we show the dynamics of the fractions of sensitive and resistant cells over time for different seeding ratios. Shown are the experimental results and simulations of (1). Clearly, while some general trends are common between the experimental data and the simulations, the fit is not optimal. For example, it takes about half the simulation time (50 hours) for the simulations to begin following the general growth trend of the data. Intriguingly, the MV model, (2), produces a worse fit to the experimental data than model (1), [9].

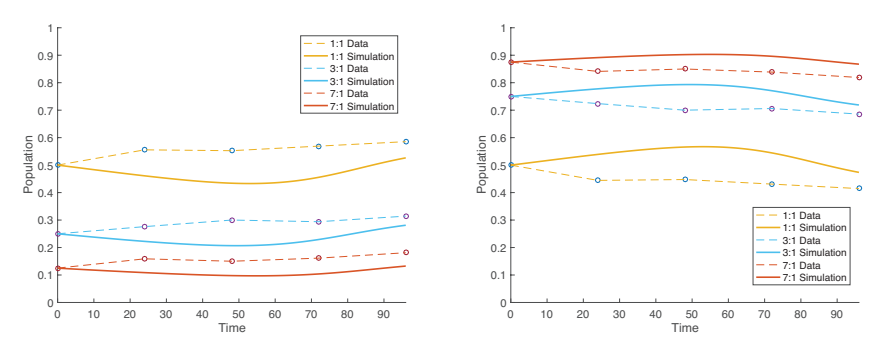


Fig. 1 Fractions of resistant (left) and sensitive (right) cells over time. Dots correspond to the experimental data of [9]. Solid lines are simulations of the model (1) of [9].

Our goal in this paper is to develop a new mathematical model for the transfer of drug resistance between cancer cell subpopulations that will provide a better fit to the experimental data of [9]. Since neither the experiments nor models of [9] include a drug, we propose a model that incorporates no action of a drug. Building on the idea of separating the cancer cells into three subtypes: sensitive, resistant, and temporary resistant, we aim at providing a more accurate model by better capturing the cancer growth dynamics. Accordingly, we incorporate the three subpopulations into a cancer growth model of Greene *et al.* [14]. This model considers cells in three states: quiescent, proliferating, and apoptotic, with transition rates that depend on the cellular density. The model was shown in [14] to provide an accurate fit to the growth dynamics of OVCAR-8, an ovarian cancer cell line. By incorporating drug resistance and a mechanism of resistance transfer into the model of [14] we provide a better match to the NCI-H460 experimental data of [9].

The structure of this paper is as follows: In section 2 we derive our new model for the P-gp transfer between cancer cells. Simulations of the model and a sensitivity study of the model parameters are shown in section 3. Since the model (1) produces more accurate results than (2), we use (1) as the reference model to which we compare our results. Concluding remarks are provided in section 4.

2 A model of P-gp transfer between cancer cells

Our starting point is the cancer growth model of Greene $et\ al.$ [14]. In this model, cancer cells are divided into three compartments: proliferating (P), quiescent (Q), and apoptotic (A) cells (see Fig. 2). The transition rates between the compartments are assumed to depend on the cellular density. Quiescent cells can either remain quiescent, start proliferating, or commit apoptosis. Proliferating cells complete the cell cycle unless they transition to apoptosis. Once the cell cycle is completed and a cell divides, both cells transition to the quiescent compartment. Once a cell commits to apoptosis, it stays in the apoptotic compartment until it dies. The duration of the cell-cycle is assumed to be normally distributed, and the time spent in the apoptotic cycle follows a gamma distribution. The model was designed to predict variations in growth as a function of the intrinsic heterogeneity originating from the varying duration of the cell-cycle and apoptosis. The model parameters were fitted in [14] to experimental data coming from OVCAR-8, an ovarian cancer cell line. However, the model is generic and could be used to describe the growth of other cancers.

To describe resistance transfer during cancer growth, we incorporate drug resistance into the PQA model of [14]. We split the quiescent compartment, Q, into sensitive (S_q) and resistant (R_q) subtypes. The proliferative compartment, P, is also divided into sensitive (S_p) and resistant (R_p) cells. In addition, the proliferative compartment also includes a temporarily resistant phenotype (T_p) . Similarly to the original PQA model, we leave the apoptotic stage as a single compartment since we assume that cells that enter apoptosis are committed to it. In our model the transfer of P-gp happens as the quiescent cells start proliferating. We assume that once cells have begun proliferating they maintain their phenotype. We define ξ to be the fraction of sensitive quiescent cells that become temporarily resistant as they transition to a proliferating state. Since P-gp transfer only leads to temporary resistance we stipulate that the progeny of temporarily resistant cells are sensitive cells. The amount of P-gp in a temporarily resistant proliferating cell is divided between the daughter cells so we consider both offsprings to be sensitive. Clearly, a more accurate model can include a larger range of resistance levels (temporary or permanent). With the rather limited experimental data at our disposal, we prefer the simpler approach presented here. A diagram corresponding to our model is shown in Fig. 3.

Two equivalent model formulations were introduced in [14]: a stochastic agent-based model, and an integro-differential (IDE) model. In this paper we choose to work with the IDE model and extend it to incorporate drug resistance. Our model equations are written as a system of six IDEs. The first two equations provide the

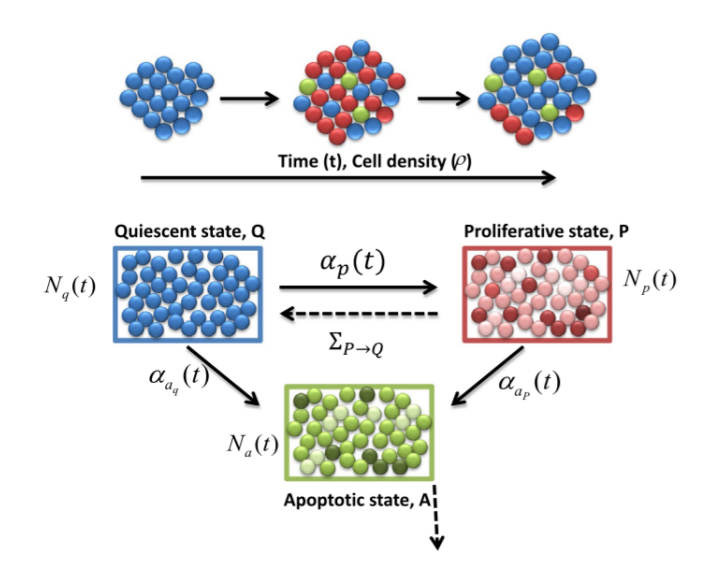


Fig. 2 Diagram representing the PQA model from [14]. Here, P denotes the proliferative compartment, with $N_P(t)$ cells at time t. Proliferating cells can either transition to apoptosis, A, or to quiescence Q, upon completion of the cell-cycle. At time t there are $N_A(t)$ apoptotic cells and $N_Q(t)$ quiescent cells. Quiescent cells can either transition to P with rate $\alpha_p(t)$, or to A with rate $\alpha_{a_q}(t)$. The implicit transition rates due to the completion of the cell cycles are shown in dashed lines.

dynamics of the quiescent cells:

$$\frac{dS_{q}}{dt} = -\alpha_{sp}S_{q}(t) - \alpha_{as_{q}}S_{q}(t)
+ 2\int_{0}^{t} f_{p}(t - t_{*}; \mu_{1}, \sigma_{1})(1 - \xi)\alpha_{sp}S_{q}(t_{*}) \left(1 - \int_{t_{*}}^{t} \alpha_{as_{p}}(s)ds\right)dt_{*}
+ 2\int_{0}^{t} f_{p}(t - t_{*}; \mu_{2}, \sigma_{2})\xi\alpha_{sp}S_{q}(t_{*}) \left(1 - \int_{t_{*}}^{t} \alpha_{as_{p}}(s)ds\right)dt_{*},$$

$$\frac{dR_{q}}{dt} = -\alpha_{rp}R_{q}(t) - \alpha_{ar_{q}}R_{q}(t)
+ 2\int_{0}^{t} f_{p}(t - t_{*}; \mu_{2}, \sigma_{2})\alpha_{rp}R_{q}(t_{*}) \left(1 - \int_{t_{*}}^{t} \alpha_{ar_{p}}(s)ds\right)dt_{*}.$$
(3)

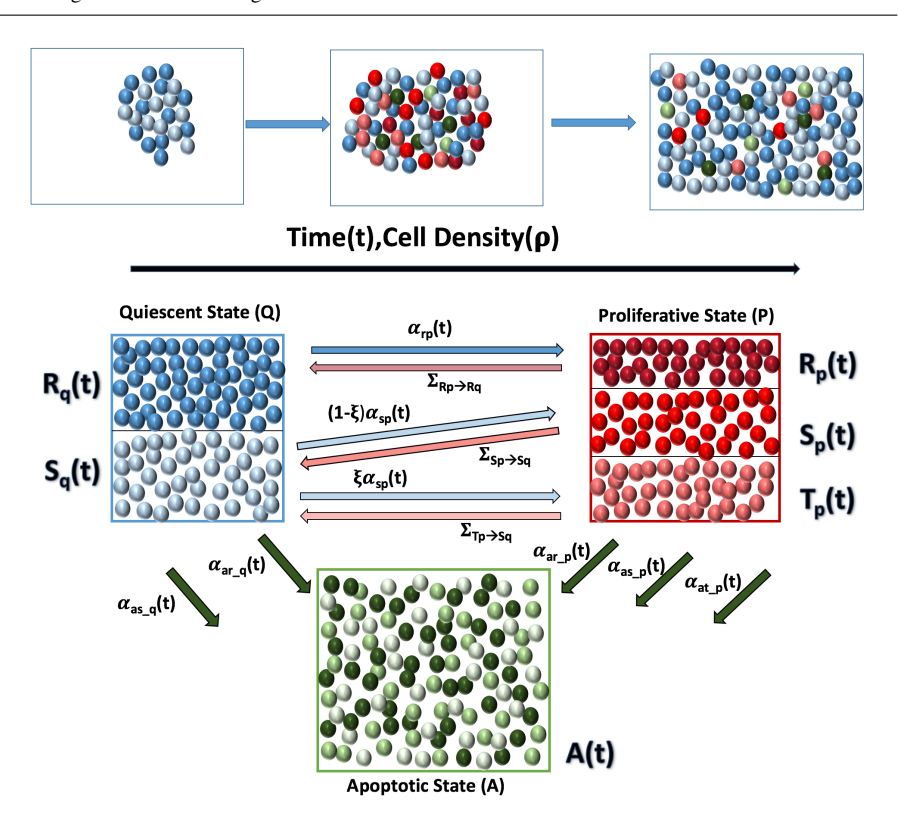


Fig. 3 Diagram representing the proposed model (3)–(5). The quiescent cells, Q, are divided into two types: resistant quiescent cells, $R_q(t)$, sensitive quiescent cells, $S_q(t)$. The proliferating cells, P, are divided into three compartments: resistant proliferating cells, $R_p(t)$, temporary resistant proliferating cells, $T_p(t)$, and sensitive proliferating cells, $S_p(t)$. Resistant proliferating cells become resistant quiescent cells upon completing the cell cycle. Sensitive and temporary resistant proliferating cells become sensitive quiescent cells when they complete the cell cycle. Proliferating and quiescent cells may become apoptotic cells, a compartment they leave only when they die. The time spent in the proliferating cycle is normally distributed with parameters that may vary depending on whether the proliferating cells are resistant or not.

Three equations follow the dynamics of proliferating cells:

$$\begin{split} \frac{dS_{p}}{dt} &= (1 - \xi)\alpha_{sp}S_{q}(t) - \alpha_{as_{p}}S_{p}(t) \\ &- \int_{0}^{t} f_{p}(t - t_{*}; \mu_{1}, \sigma_{1})(1 - \xi)\alpha_{sp}S_{q}(t_{*}) \left(1 - \int_{t_{*}}^{t} \alpha_{as_{p}}(s)ds\right)dt_{*}, \\ \frac{dR_{p}}{dt} &= \alpha_{rp}R_{q}(t) - \alpha_{ar_{p}}R_{p}(t) \\ &- \int_{0}^{t} f_{p}(t - t_{*}; \mu_{2}, \sigma_{2})\alpha_{rp}R_{q}(t_{*}) \left(1 - \int_{t_{*}}^{t} \alpha_{ar_{p}}(s)ds\right)dt_{*}, \\ \frac{dT_{p}}{dt} &= \xi \alpha_{sp}S_{q}(t) - \alpha_{at_{p}}T_{p}(t) \\ &- \int_{0}^{t} f_{p}(t - t_{*}; \mu_{2}, \sigma_{2})\xi \alpha_{sp}S_{q}(t_{*}) \left(1 - \int_{t_{*}}^{t} \alpha_{at_{p}}(s)ds\right)dt_{*}. \end{split}$$

$$(4)$$

A sixth equation describes the dynamics of apoptotic cells:

$$\frac{dA}{dt} = \alpha_{as_q} S_q(t) + \alpha_{ar_q} R_q(t) + \alpha_{as_p} S_p(t) + \alpha_{ar_p} R_p(t) + \alpha_{at_p} T_p(t)
- \int_0^t f_a(t - t_*) \alpha N(t_*) dt_*.$$
(5)

The first equation in (3) follows the dynamics of the sensitive quiescent cells, S_q . The first term on the RHS, $-\alpha_{sp}S_q(t)$, corresponds to the fraction of cells lost as a result of the transition to the proliferative compartment P. This term encompasses cells that stay sensitive and those that become temporarily resistant. The second term, $\alpha_{as_q}S_q(t)$, corresponds to the loss as a result of the transition to apoptosis. The integral term

$$2\int_0^t f_p(t-t_*;\mu,\sigma)\alpha_{sp}S_q(t_*)\left(1-\int_{t_*}^t \alpha_{as_p}(s)ds\right)dt_*$$

corresponds to the increase in S_q due to the progeny of the sensitive proliferating cells. We assume that all proliferating cells originated from quiescent cells, so $\alpha_{sp}S_q(t*)$ includes all sensitive proliferating cells. There are two such terms, the first (with $1-\xi$) corresponds to sensitive proliferating cells that competed their proliferating cycle (hence the factor of 2 in front of the integral). The second term (with ξ) corresponds to temporary resistant cells that completed their proliferation cycle and became sensitive quiescent cells. We assume that the time spent in the proliferative compartment is normally distributed with mean μ and standard deviation σ , both measured in hours,

$$f_p(t;\mu,\sigma) = \frac{1}{\sqrt{2\pi}\sigma} e^{-\frac{(t-\mu)^2}{2\sigma^2}}.$$
 (6)

The term $1 - \int_{t_*}^t \alpha_{as_p}(s) ds$ describes the cells in the cell cycle that did not move to apoptosis before completing the proliferation cycle, where t corresponds to the time cells entered the proliferating compartment. Overall, the full integral accounts for the progeny for the proliferating cells whose time spent in the cell cycle has come to an end. The somewhat complex bookkeeping in this model (expressed by the integral terms) is due to assuming a distribution on the time cells may take to proliferate (and die), as opposed to the more standard approach of assuming that these values are constant. We allow the proliferation time, characterized by the parameters of the normal distribution, μ and σ , to differ between the resistant and sensitive populations since resistant cells may have a slower proliferation rate [6]. If these parameters are assumed to be identical for resistant and sensitive cells, both integrals terms can be combined into one term.

The second equation in (3) describes the dynamics of the resistant quiescent population, R_q . The RHS is similar to the first equation, with a loss term due to transition into the cell cycle and another loss term due to transition to apoptosis. Since we assume that these cells exhibit a resistant genotype we do not allow them to lose their resistance and so the integral term represents the progeny from all the resistant cells in the cell cycle that have their time span end at a certain time t.

Similar equations are provided for the three types of cells in the proliferative compartment, described in (4). The first term on the RHS of the first equation for the

sensitive proliferative population, S_p , represents the fraction of sensitive quiescent cells that started proliferating but stayed sensitive and did not acquire any temporary resistance. We include an apoptotic term and the same integral seen in (3), representing the end of the cell cycle in which each proliferating cell that has not transitioned into apoptosis divides into two new quiescent cells. The second equation, for the resistant proliferating cells, R_p , includes a transition term from resistant quiescent to resistant proliferative and another term representing transition to apoptosis term with the integral from the second equation in (3) showing the loss due to division at the end of the cell cycle, as cells transition to the resistant quiescent cells compartment. The third equation, for the temporary resistant proliferating cells, T_p , has the same three types of terms, with ξ multiplying the transition term from sensitive quiescent showing the fraction of cells that acquired temporary resistance.

Finally, (5) describes the apoptotic compartment. Once cells start apoptosis we no longer distinguish between resistant or sensitive cells. Equation (5) includes the five growth terms that correspond to the transitions from all compartments in (3)–(4). The length of time spent in apoptotic state is assumed to be a Gamma distribution,

$$f_a(t) = \frac{\lambda^{\omega}}{\Gamma(\omega)} t^{\omega - 1} e^{-\lambda t}, \tag{7}$$

with λ and γ the rate and shape parameters of the apoptotic process and $\Gamma(\cdot)$ the gamma function. Once cells complete the time committed to apoptosis, they are removed from the system. The integral term describes this removal for all cells that die at time t. In this term we denote the total loss by $\alpha N(t) := \alpha_{as_q} S_q(t) + \alpha_{ar_q} R_q(t) + \alpha_{as_p} S_p(t) + \alpha_{ar_p} R_p(t) + \alpha_{at_p} T_p(t)$.

The transitions rates from [14] are functions of $\beta(\rho)$ and d, the equilibrium fraction of proliferating cells and the fraction in apoptosis, which we take to be constant. We set β_m and ρ_m as the maxima for β , and ρ , respectively, and define

$$\beta(\rho) = \begin{cases} \beta_m e^{-a(\rho - \rho_m)^2/\rho(1+\varepsilon-\rho)^2} & \text{if } 0 < \rho < 1+\varepsilon, \\ 0 & \text{otherwise.} \end{cases}$$
 (8)

Here, ε is a parameter governing the shape of $\beta(\rho)$, and

$$a = \frac{\varepsilon \log(\beta_m/d)}{(1 - \rho_m)^2}. (9)$$

We define the transitions $\alpha_{sp}(t)$ and $\alpha_{rp}(t)$ as the rates from sensitive quiescent to sensitive or temporarily resistant proliferating and resistant quiescent to resistant proliferating, respectively. We make the assumption that P-gp expression is independent of the transition. Hence, we set $\alpha_{sp}(t) = \alpha_{rp}(t)$. The intrinsic death terms from quiescent to apoptotic are $\alpha_{as_q}(t)$ and $\alpha_{ar_q}(t)$, with the death terms from proliferative to apoptotic being $\alpha_{as_p}(t), \alpha_{ar_p}(t)$, and $\alpha_{at_p}(t)$. We again consider no effect of P-gp transfer on these terms and thus have $\alpha_{as_q}(t) = \alpha_{ar_q}(t)$ and $\alpha_{as_p}(t) = \alpha_{ar_p}(t) = \alpha_{ar_p}(t)$

 $\alpha_{at_p}(t)$. These transition rates are shown below.

$$\alpha_{sp}(t) = \alpha_{rp}(t) = c \frac{(\beta(\rho(t))N(t) - P(t))_{+}}{Q(t)}, \qquad (10)$$

$$\alpha_{as_p}(t) = \alpha_{ar_p}(t) = \alpha_{at_p}(t) = c\gamma \frac{(dN(t) - A(t))_+}{P(t)}, \tag{11}$$

$$\alpha_{as_q}(t) = \alpha_{ar_q}(t) = c(1 - \gamma) \frac{(dN(t) - A(t))_+}{Q(t)}.$$
 (12)

Here, Q(t), P(t), and A(t) are the total number of cells in each respective compartment and N(t) = Q(t) + P(t) + A(t) with $\rho(t) = N(t)/K$ for a carrying capacity K. The transition from Q to P is a function of the difference between the current proliferative population, P(t), and the desired (or equilibrium) proliferative population, $\beta(\rho(t))N(t)$. Similarly, the transitions into apoptosis are functions of the difference between current apoptotic population A(t), and the desired fraction in apoptosis dN(t), where d is taken to be a small constant < 0.05. c is the cellular reaction rate and γ describes the rate difference between the proliferating cells and quiescent cells when entering apoptosis.

3 Results

3.1 Numerical Methods

We use a four-step explicit Adams-Bashforth (AB) method to approximate solutions of the system (3)–(5). This solver is chosen since it does not require temporary intermediate values, which simplifies the calculations due to the presence of the integral terms. The method can be written as

$$y_{n+1} = y_n + \frac{\Delta t}{24} (55f_n - 59f_{n-1} + 37f_{n-2} - 9f_{n-3}), \tag{13}$$

with lower degree AB methods for the first 3 steps. Integrals of the form

$$\int_{0}^{t} h_{1}(t, t_{*}) \left(1 - \int_{t_{*}}^{t} h_{2}(s) ds\right) dt_{*}$$
(14)

are discretized using the same time steps used with the AB method (13). If we denote

$$I(t,t_*) = \int_t^t h_2(s)ds,$$

we can approximate $I(t + \Delta t, t_*)$ with

$$I(t + \Delta t, t_*) = \int_{t_*}^{t + \Delta t} h_2(s) ds = \int_{t_*}^{t} h_2(s) ds + \int_{t}^{t + \Delta t} h_2(s) ds$$

$$\approx \int_{t_*}^{t} h_2(s) ds + h_2(t) \Delta t = I(t, t_*) + h_2(t) \Delta t.$$
(15)

Table 1 Parameter Values & Descriptions

Parameter	Range	Description	Reference
t	[0,180] (hours)	Time	[9]
μ_1	[10,∞) (hours)	Mean length of (sensitive) cell cycle	[14]
σ_{l}	[0,10] (hours)	Standard deviation of (sensitive) cell cycle	[14]
μ_2	[12,∞) (hours)	Mean length of (resistant) cell cycle	[14]
σ_2	[0,10] (hours)	Standard deviation of (sensitive) cell cycle	[14]
ω	4.9436	Shape parameter of entire apoptotic process	[14]
λ	0.19117 (per hour)	Rate parameter of entire apoptotic process	[14]
$\rho(t)$	$[0,\infty)$	Density of cells at time t	[14]
K	7.5×10^5	Carrying capacity	[9]
d	[0.01,0.05]	Fraction of cells in apoptosis	[14]
$\beta(ho)$	[0,1]	Fraction in cell cycle as a function of density	[14]
eta_m	[0,1]	Maximum of $\beta(\rho)$	[14]
$ ho_m$	[0,1]	Maximizing density of $oldsymbol{eta}(ho)$	[14]
ε	$[0,\infty)$	Parameter governing shape of $oldsymbol{eta}(ho)$	[14]
c	$[0,\infty)$ (per hour)	Cellular reaction rate	[14]
γ	[0,1]	Rate difference between $lpha_{ap}$ and $lpha_{aq}$	[14]
ξ	[0,1]	Fraction of cells becoming temporarily resistant	

Equation (15) requires only one function evaluation. The complete integral (14) is then evaluated with a composite trapezoidal rule on a uniform grid:

$$\int_{0}^{t} h_{1}(t, t_{*}) \left(1 - \int_{t_{*}}^{t} h_{2}(s) ds\right) dt_{*} \approx \frac{\Delta t}{2} \sum_{k=1}^{N} \left(h_{1}(t, t_{k})(1 - I(t, t_{k}))\right) + h_{1}(t, t_{k+1})(1 - I(t, t_{k+1})),$$
(16)

with t_k the kth point and N the size of the discretization.

In our simulations, we optimized the model parameters using Matlab's nonlinear least squares function, fitting the solution of (3)–(5) to the experimental data of [9]. We set d=0.03, which corresponds to the same fraction of cells in apoptosis from [14]. The full list of parameters and their ranges is given in Table 1. The optimal values used in the simulations are given in Table 2 for the case in which resistant cells and sensitive cells have different growth parameters, and in Table 3 for the case when the growth parameters are identical for both sensitive and resistant cells.

Table 2 Parameters values used in simulations with different growth parameters for the sensitive and resistant cells

Parameter	μ_1	σ_{l}	μ_2	σ_2	ω	λ	K
Value	10.0258	9.2818	12.0033	5.8467	4.9436	0.19117	7×10^5
Parameter	d	eta_m	$ ho_m$	ε	c	γ	ξ
Value	0.03	0.8	0.0458	0	15.4753	0.8331	0.0412

Table 3 Parameters Values Used in Simulations with identical growth parameters for the sensitive and resistant cells

Parameter	μ_1	σ_1	μ_2	σ_2	ω	λ	K
Value	10.2365	4.3263	10.2365	4.3263	4.9436	0.19117	7×10^5
Parameter	d	eta_m	$ ho_m$	ε	c	γ	ξ
Value	0.03	0.8	0.2	0.2346	1.6732	0.5011	0.4828

3.2 Simulations

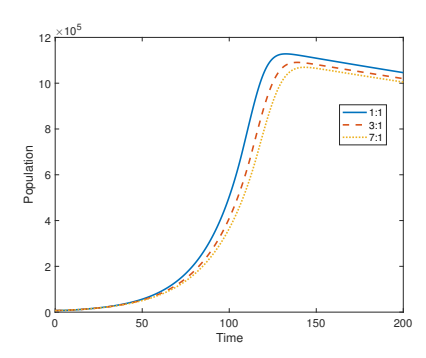


Fig. 4 The dynamics of the total population of resistant and sensitive cells over 200 hours simulated with (3)–(5). We consider the three initial ratios of sensitive to resistant cells: 1:1, 3:1, and 7:1.

Our first simulations show the total population of sensitive and resistant cells over time for three different initial conditions. Following the setup of [9] we run separate simulations for a 1:1, 3:1, and 7:1 initial ratio of sensitive to resistant cells. The resistant subtype, as described in [9], are cells that have been given Doxorubicin for three months and survived. At time t=0 all cells are assumed to be quiescent. Fig. 4 shows growth up to a carrying capacity and then a small decline, which compares well to the data shown in [9]. The trend of the population growth is similar in all three cases.

We next look at the how the fractions of sensitive and resistant cells change over time. The results are shown in Fig. 5. We compared simulations of our model (3)–(5) with simulations of the model of [9] given by (1). The simulations results are plotted on top of the experimental data of [9]. A comparison between the results produced by both models shows that the new model (3)–(5) provides a substantially better match to the experimental data over the simulated 96 hours, compared with the model (1), both in terms of the absolute error, as well as the overall trend. We see an early inflection point in our model due to the faster proliferation rate of the sensitive cells. Initially the growth of the sensitive cell fraction outpaces the resistant cell fraction. After about 12 hours the resistant cells begin to catch up. Then the transfer of resistance contributes to a rise in the fraction of resistant cells.

To verify that the results are not due to overfitting sparse data, we significantly oversampled the data, which is straightforward due to its monotonicity, and repeated all simulations. The fits we obtained using the oversampled data were nearly identical to those obtained with the experimental dataset.

We test the sensitivity of the model (3)–(5) to changes in four of the parameters, d, c, ε , and ξ . Fig. 6 shows how the overall population varies when d, c, and ε , respectively, are changed. We ran simulations to compare how the sensitive and resistant fractions change but these result with only negligible changes so we focus on total cell population. Changes to d, the parameter governing the fraction of cells in apoptosis, are shown in the top left graph in Fig. 6. There is a small effect on the overall population once it has reached carrying capacity with a larger death parameter correlating with a faster decline but the system overall does not change much as d changes. The cellular reaction rate c amplifies the magnitude of cells moving from quiescent stage into the cell cycle. The simulation shown in the top right graph in Fig. 6 confirms that a low c value correlates with slower growth. However, for larger values of c, the growth is mostly independent of c. The parameter ε governs the shape of $\beta(\rho)$, the equilibrium, or desired, amount of cells in the cell-cycle. The bottom left graph in Fig. 6 demonstrates that the total population is sensitive to changes in ε . While the sensitive and resistant fractions remain consistent, any deviation from $\varepsilon = 0$ leads to a significant decrease in the overall growth. $\varepsilon = 0$ implies that $\beta(\rho) = \beta_m$, a constant. This corresponds to a lack of dependence on density. We expect this to be the best fit as both the model and the experimental data address a local phenomenon.

The parameter ξ , which governs the fraction of sensitive quiescent cells that become temporarily resistant as they enter the cell cycle, is the final parameter we varied. Resistant cells proliferate at a slower rate but we see that the difference is not enough to induce change on the overall population. However, there is a shift in the sensitive and resistant fractions, as would be expected. Fig. 7 shows the population and the two fractions while Fig. 8 shows a zoomed on version of Fig. 7 to highlight the shift towards more resistance as ξ is raised. The larger ξ is, the more cells become temporarily resistant and so the overall resistant fraction rises.

We also ran simulations in which we allowed the sensitive and resistant cells to have the same growth parameters (i.e., a normal distribution with identical mean and standard deviations for the cell cycle length). Without the slower proliferation our optimized parameters have a much larger value for ξ , the fraction of sensitive quiescent cells that become temporarily resistant. In these simulations we have almost

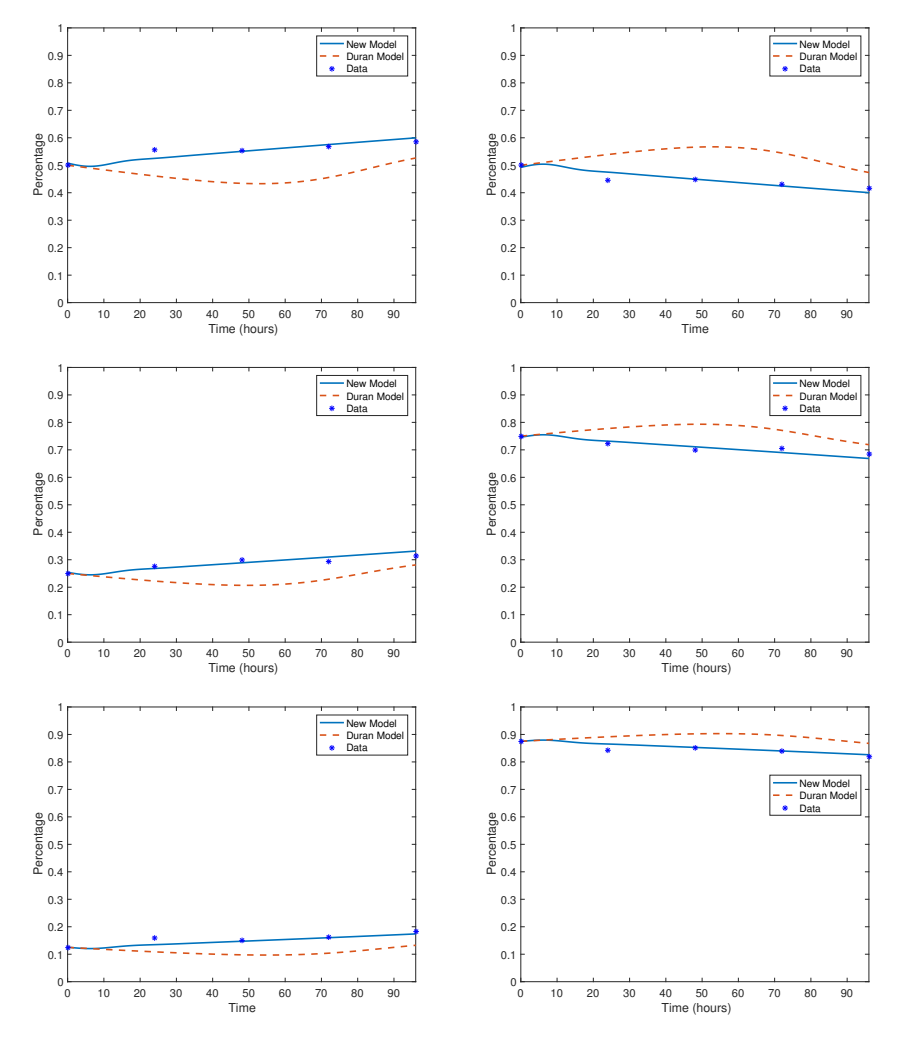


Fig. 5 Fractions of resistant (left) and sensitive (right) cells over time. Top: initial ratio 1:1. Middle: initial ratio 3:1. Bottom: initial ratio 7:1. Dots correspond to the experimental data of [9]. Dashed lines are simulations with the model (1) of [9]. Solid lines are simulations of (3)–(5).

half of them becoming resistant ($\xi = 0.4828$). The results of these simulations are shown in Fig. 9 (compare with Fig. 5 where resistant cells are assumed to grow slower than the sensitive cells). Even in this case, our model (3)–(5) provides a better match in capturing the trend of the data compared with the model of [9].

We note that the parameters are optimized based on the available experimental data that was collected over the first 96 hours. When simulating our model beyond 96 hours with identical growth distributions for the sensitive and the resistance cells, the fractions of sensitive and resistant cells trend back towards their initial values. The

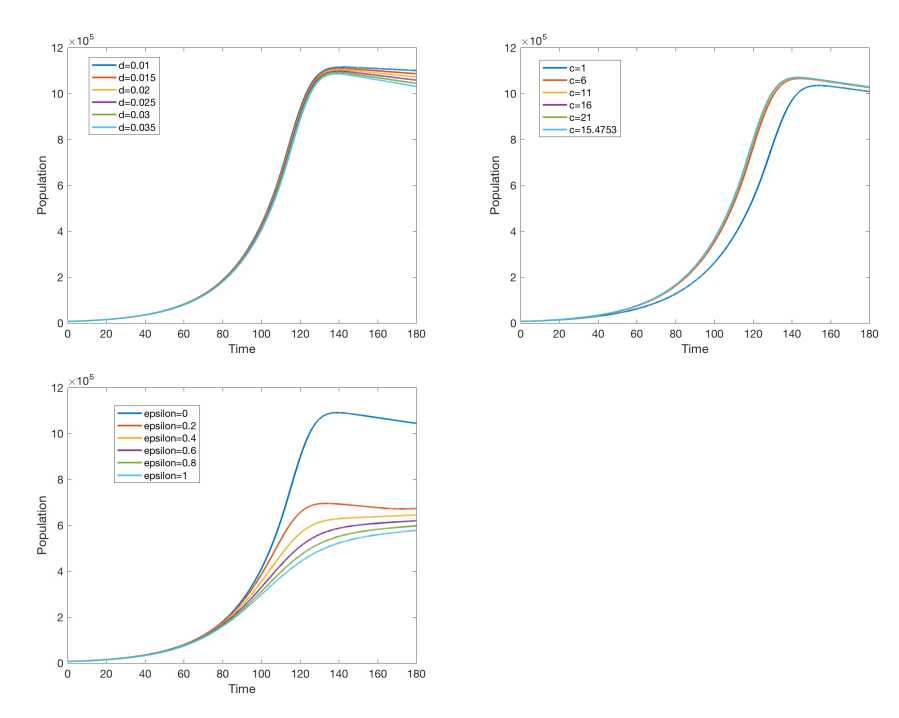


Fig. 6 Sensitivity study of (3)–(5) for the case of an initial sensitive to resistant ratio of 3:1. All graphs show the total cell population over time. Top Left: varying d, the fraction of cells in apoptosis. Top Right: varying c, the cellular reaction rate that governs the transition from quiescent to proliferative. Bottom: varying ε , the shape parameter for $\beta(\rho)$.

model (1) exhibits a limit dynamics in which the sensitive and resistant cells settle towards equilibrium values albeit values that are different than the initial distribution.

It is easy to understand the reason for this asymptotic behavior when the growth distributions of sensitive and resistant cells are identical. In this case, we can assume that R_p changes at a similar rate to $S_p + T_p$. When the carrying capacity is approached, $\beta(\rho)$ gets increasingly small. This means that the transition rates from quiescence to the proliferative compartment shrink. Once all the temporarily resistant proliferating cells divide into sensitive quiescent cells, the transition rates are too small to repopulate T_p . The overwhelming majority of cells are quiescent, either resistant or sensitive. When temporary resistant cells make up a small fraction of the population, the asymptotic distribution of cells reverts to the initial values. This can all be avoided by allowing the resistant population to proliferate at a slower rate than the sensitive cells, which is a biologically solid assumption [6].

4 Conclusions

Mathematical models of the mechanisms of cellular growth may assist in studying and understanding the emergence and evolution of MDR. The cell-to-cell transfer of P-gp and its effect have not been extensively studied by the mathematical community.

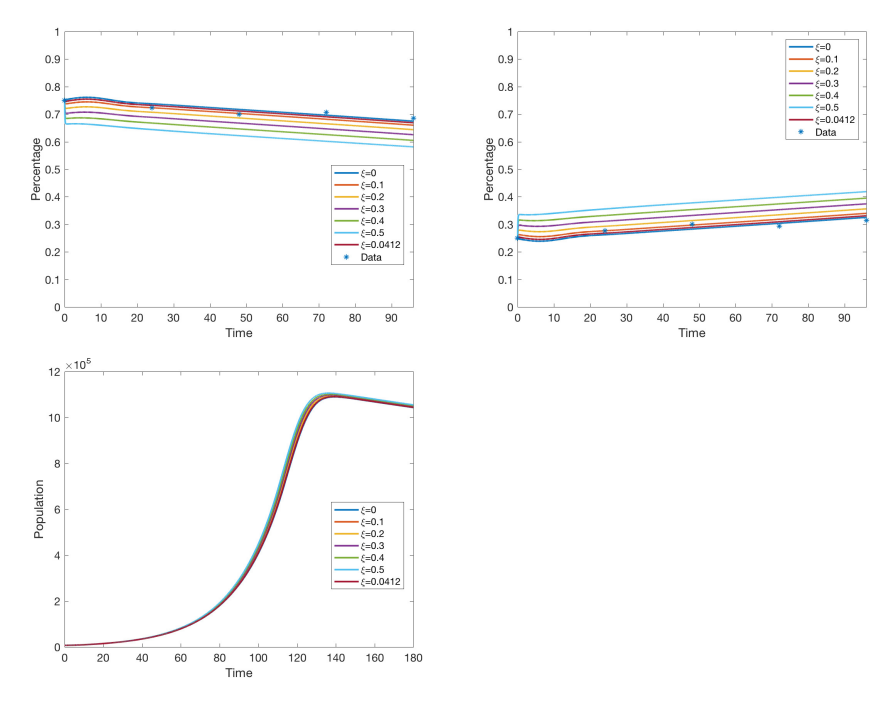


Fig. 7 Top Left: Fraction of sensitive cells as ξ , the fraction of sensitive quiescent cells that transition to temporarily resistant when in the proliferative state, varies. Top Right: Fraction of resistant cells as ξ varies. Bottom: Total Population as ξ varies.

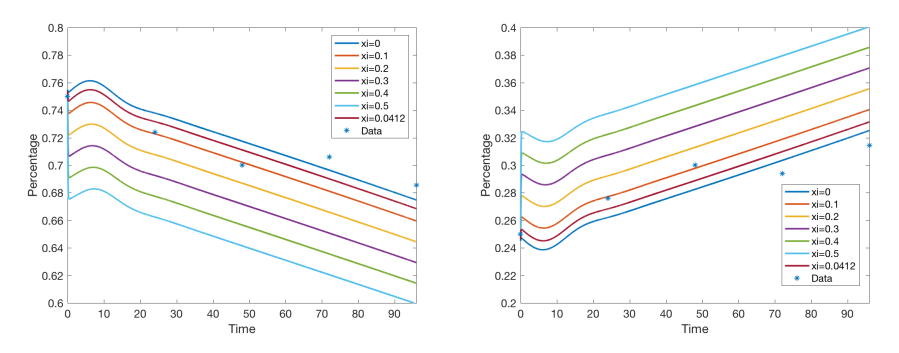


Fig. 8 Left: A close up for the fraction of sensitive cells as ξ , the fraction of sensitive quiescent cells that transition to temporarily resistant when in the proliferative state, varies. Right: A close up for the fraction of resistant cells as ξ varies.

In this paper we propose a model for the resistance transfer between cells. Our model assumes that cells are either quiescent, proliferative, or in the apoptotic stage. Cells in the quiescent and proliferative stages are designated either resistant or sensitive, with an extra compartment for temporarily resistant proliferative cells. We assume that a certain fraction of sensitive cells become temporarily resistant due to

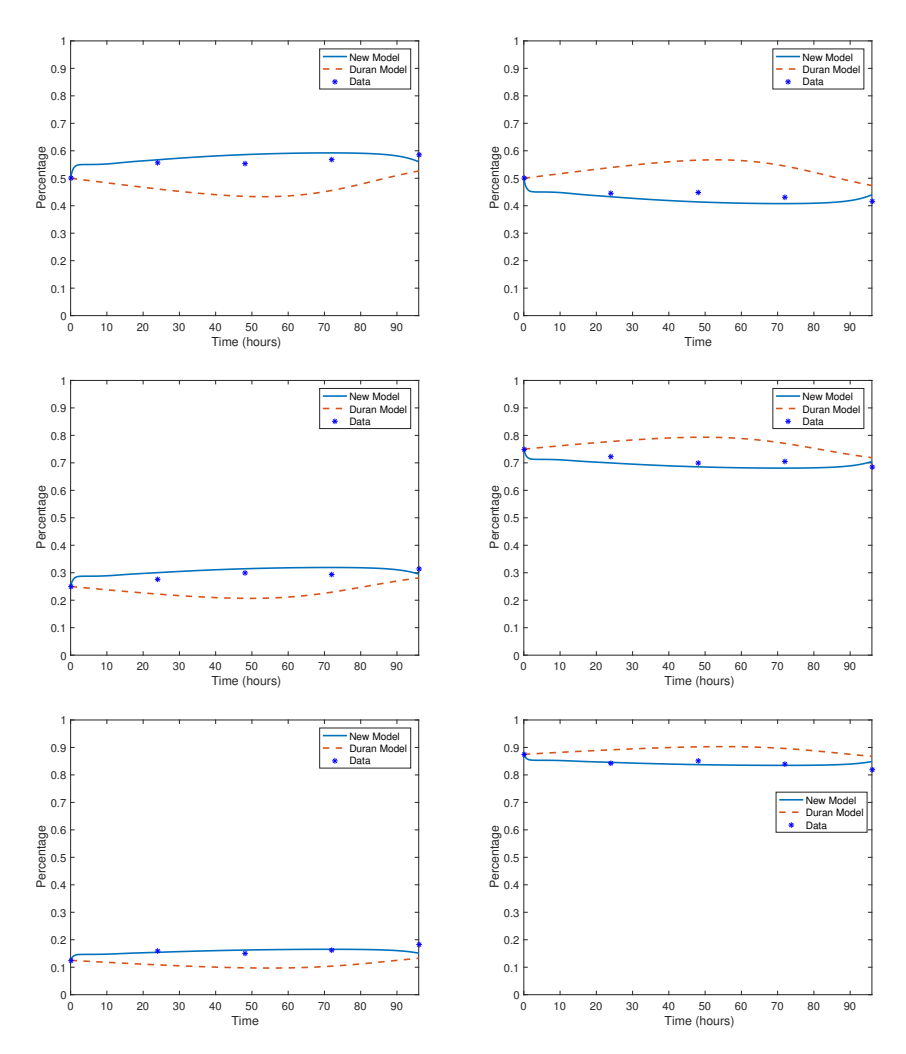


Fig. 9 Fractions of resistant (left) and sensitive (right) cells over time assuming identical growth parameters for the sensitive and the resistant cells. The parameters used in this figure are given in Table 3. Top: initial ratio 1:1. Middle: initial ratio 3:1. Bottom: initial ratio 7:1. Dots correspond to the experimental data of [9]. Dashed lines are simulations with the model (1) of [9]. Solid lines are simulations of (3)–(5).

P-gp transfer as they become proliferative and enter the cell cycle. This model is an extension of the cancer growth model of Greene *et al.* [14] to which we incorporated drug resistance.

We fit our model to the experimental data from [9] and show that the more detailed description of the growth dynamics in our model provides a better fit to the experimental data than the fit that can be obtained using the original model of [9]. We demonstrate that a better match to the experimental data is obtained when resistant cells are allowed to grow at a different rate than the sensitive cells. The best fit is

obtained when the resistant cells grow more slowly than the sensitive cells, which is consistent with known experimental data.

Acknowledgements The work of DL was supported in part by the NSF under Grant Number DMS-1713109, by the John Simon Guggenheim Memorial Foundation, by the Simons Foundation, and by the Jayne Koskinas Ted Giovanis Foundation.

References

- Cancer facts & figures 2016. URL https://www.cancer.org/research/ cancer-facts-statistics/all-cancer-facts-figures/cancer-facts-figures-2016.
- 2. Ambudkar, S.V., Sauna, Z.E., Gottesman, M.M., Szakacs, G.: A novel way to spread drug resistance in tumor cells: functional intercellular transfer of p-glycoprotein (abcb1). Trends in pharmacological sciences **26**(8), 385–387 (2005)
- Balaj, L., Lessard, R., Dai, L., Cho, Y.J., Pomeroy, S.L., Breakefield, X.O., Skog, J.: Tumour microvesicles contain retrotransposon elements and amplified oncogene sequences. Nature communications 2, 180 (2011)
- Borst, P., Evers, R., Kool, M., Wijnholds, J.: A family of drug transporters: the multidrug resistanceassociated proteins. Journal of the National Cancer Institute 92(16), 1295–1302 (2000)
- Breier, A., Gibalova, L., Seres, M., Barancik, M., Sulova, Z.: New insight into p-glycoprotein as a drug target. Anti-Cancer Agents in Medicinal Chemistry (Formerly Current Medicinal Chemistry-Anti-Cancer Agents) 13(1), 159–170 (2013)
- Brimacombe, K.R., Hall, M.D., Auld, D.S., Inglese, J., Austin, C.P., Gottesman, M.M., Fung, K.L.: A
 dual-fluorescence high-throughput cell line system for probing multidrug resistance. Assay and drug
 development technologies 7(3), 233–249 (2009)
- Cordon-Cardo, C., O'Brien, J., Boccia, J., Casals, D., Bertino, J., Melamed, M.: Expression of the multidrug resistance gene product (p-glycoprotein) in human normal and tumor tissues. Journal of Histochemistry & Cytochemistry 38(9), 1277–1287 (1990)
- Davidson, A.L., Dassa, E., Orelle, C., Chen, J.: Structure, function, and evolution of bacterial atpbinding cassette systems. Microbiology and Molecular Biology Reviews 72(2), 317–364 (2008)
- Durán, M.R., Podolski-Renić, A., Álvarez-Arenas, A., Dinić, J., Belmonte-Beitia, J., Pešić, M., Pérez-García, V.M.: Transfer of drug resistance characteristics between cancer cell subpopulations: A study using simple mathematical models. Bulletin of mathematical biology 78(6), 1218–1237 (2016)
- Fodale, V., Pierobon, M., Liotta, L., Petricoin, E.: Mechanism of cell adaptation: when and how do cancer cells develop chemoresistance? The Cancer Journal 17(2), 89–95 (2011)
- 11. Ford, J.M., Yang, J.M., Hait, W.N.: P-glycoprotein-mediated multidrug resistance: experimental and clinical strategies for its reversal. In: Drug Resistance, pp. 3–38. Springer (1996)
- 12. Geoffrey, M.C., Robert, E., et al.: The cell: a molecular approach. Boston University, Sunderland (2000)
- Gillet, J.P., Gottesman, M.M.: Mechanisms of multidrug resistance in cancer. Multi-drug resistance in cancer pp. 47–76 (2010)
- Greene, J.M., Levy, D., Fung, K.L., Souza, P.S., Gottesman, M.M., Lavi, O.: Modeling intrinsic heterogeneity and growth of cancer cells. Journal of theoretical biology 367, 262–277 (2015)
- 15. Jackson, T.L., Byrne, H.M.: A mathematical model to study the effects of drug resistance and vasculature on the response of solid tumors to chemotherapy. Mathematical biosciences **164**(1), 17–38 (2000)
- Juranka, P., Zastawny, R., Ling, V.: P-glycoprotein: multidrug-resistance and a superfamily of membrane-associated transport proteins. The FASEB Journal 3(14), 2583–2592 (1989)
- 17. Lavi, O., Gottesman, M.M., Levy, D.: The dynamics of drug resistance: a mathematical perspective. Drug Resistance Updates **15**(1), 90–97 (2012)
- Lavi, O., Greene, J.M., Levy, D., Gottesman, M.M.: The role of cell density and intratumoral heterogeneity in multidrug resistance. Cancer research 73(24), 7168–7175 (2013)
- Leonard, G.D., Fojo, T., Bates, S.E.: The role of abc transporters in clinical practice. The oncologist 8(5), 411–424 (2003)

- Levchenko, A., Mehta, B.M., Niu, X., Kang, G., Villafania, L., Way, D., Polycarpe, D., Sadelain, M., Larson, S.M.: Intercellular transfer of p-glycoprotein mediates acquired multidrug resistance in tumor cells. Proceedings of the National Academy of Sciences of the United States of America 102(6), 1933–1938 (2005)
- Lorz, A., Lorenzi, T., Hochberg, M.E., Clairambault, J., Perthame, B.: Populational adaptive evolution, chemotherapeutic resistance and multiple anti-cancer therapies. ESAIM: Mathematical Modelling and Numerical Analysis 47(2), 377–399 (2013)
- 22. Pasquier, J., Galas, L., Boulangé-Lecomte, C., Rioult, D., Bultelle, F., Magal, P., Webb, G., Le Foll, F.: Different modalities of intercellular membrane exchanges mediate cell-to-cell p-glycoprotein transfers in mcf-7 breast cancer cells. Journal of Biological Chemistry 287(10), 7374–7387 (2012)
- 23. Pasquier, J., Magal, P., Boulangé-Lecomte, C., Webb, G., Le Foll, F.: Consequences of cell-to-cell p-glycoprotein transfer on acquired multidrug resistance in breast cancer: a cell population dynamics model. Biology direct **6**(1), 1 (2011)
- Thiebaut, F., Tsuruo, T., Hamada, H., Gottesman, M.M., Pastan, I., Willingham, M.C.: Cellular localization of the multidrug-resistance gene product p-glycoprotein in normal human tissues. Proceedings of the National Academy of Sciences 84(21), 7735–7738 (1987)
- Ueda, K., Clark, D., Chen, C., Roninson, I., Gottesman, M., Pastan, I.: The human multidrug resistance (mdr1) gene. cdna cloning and transcription initiation. Journal of Biological Chemistry 262(2), 505–508 (1987)
- 26. Weinberg, R.: The biology of cancer. Garland science (2013)